Hydration behavior of protic ionic pair of methyl ammonium formate: A comparative molecular dynamics simulation study with their conjugate neutral forms

Th. Dhileep N. Reddy, Bhabani S. Mallik*

Department of Chemistry, Indian Institute of Technology Hyderabad, Kandi-502285, Sangareddy, Tealangana, India

ABSTRACT

The structure and dynamics of methylammonium formate (MAF), methylamine (MA) and formic acid (FOR) in aqueous solution were investigated by employing classical molecular dynamics simulations. We explored the fundamental difference between charged and their corresponding conjugate neutral forms towards interactions with water molecules. Structural properties were investigated by calculating radial distribution functions, spatial distribution functions, and combined distribution functions. These properties reveal that water molecules approach the solutes in a specific direction. The hydrogen bonds formed by ionic species are stronger as compared to the neutral molecules. MA interacts through its nitrogen atom mainly whereas MAM interacts through its acidic hydrogen atoms. Dynamic properties were investigated by continuous and forward hydrogen bond lifetimes of all possible pairs as well as residence times calculated from respective autocorrelation functions. Dynamics become slow in ionic environments and profound differences in dynamics are found in case of concentrated solutions as compared to dilute solutions.

1. Introduction

Understanding solvation structure and dynamics of ions in water have fundamental importance to understand the microscopic details of the origin of the chemical reactions in solution [1,2]. Interactions between ions and water play an important role in biological processes [3]. The biological importance of the amine group is huge, which exists as a protonated form in most of the biological tissues [4]. The amino group is part of peptides and proteins and responsible for many biological functions. Water is the primary solvent in most of the biological processes and solvation of bio-relevant molecules in water is one of the most explored problems in biochemistry. Interaction between compounds containing ammonium ion and protein receptors is important in biological signal transduction processes [4]. Malfunctioning of dopamine-responsive neurons leads to many diseases such as Parkinson's, which is still challenging in medical and biological fields [5]. Alkylammonium recognition in dopamine neurotransmitters will provide one more step towards the understanding of main causes for these types of diseases. Studying alkylammonium ions interaction with ligands and water is essential [6]. Stabilization of zwitterion structures depends on the interactions between amino acids and other molecules. In biological systems, ammonium ions exhibit mainly three types of interactions;

Hydrogen bonds, cation-π interactions, ion pairs, and salt bridges. The charged methylamine can be considered as a model compound for ionic biomolecules.

Ionic liquids containing alkylammonium ions are used as alternate solvents in determining protein structure and stability [7] and in enzyme catalysis [8]. The main contribution to the interaction between ammonium ions and polar molecules is from hydrogen bonding. Many quantum chemical studies based on ammonium ions were performed to understand its structure and stability. But, alkylammonium ions were much less studied [9–11]. In the group of protonated amine (R-NH$_3^+$), methylammonium (MAM) ion (CH$_3$−NH$_3^+$) is the simplest model and is essential to study the CH$_3$−NH$_3^+$−Water hydrogen bonds (HBs) [9,12–17]. CH$_3$−NH$_3^+$ is the simplest protonated amine and is considered as amphiphilic as it contains both hydrophilic (−NH$_3^+$) and hydrophobic (−CH$_3$) moieties [18,19]. Alagona et al. from their Monte-Carlo (MC) simulations suggested that −NH$_3^+$ has the coordination number of 3.5 in aqueous solution; on average, one water molecule solvates each hydrogen atom of an ammonium group. For the hydrophobic side of MAM, the number of water molecules fluctuates between 12 and 15 depending on the first minimum [9]. Moreover, Jorgensen et al. suggested that CH$_3$-NH$_3^+$ formed four strong HBs with water molecules using optimized potentials for liquid simulations (OPLS)

* Corresponding author.
  E-mail address: bhabani@iith.ac.in (B.S. Mallik).

force fields [15]. According to molecular dynamics (MD) study, hydration numbers were reported as 3.67 and 9.33 for the hydrophilic and hydrophobic groups, respectively [16]. Car-Parrinello (CP) MD simulation study of an aqueous solution of MAM reported that 4.2 water molecules were present in the first solvation shell of the ammonium group [17]. The conjugate base form of MAM is MA, which is found in human blood, urine, and tissues [20–25]. Dunn et al. suggested from their MC simulation studies that this group has three water molecules in its first hydration shell [26]. Kusalik et al. showed that two water molecules should present to form hydrogen bonds with the amine group in its first solvation shell [27]. Hesske and Gloe showed that hydrogen bonds exist between one water molecule and nitrogen of MA and also existed between two water molecules and two hydrogen atoms of the amine group [17]. Rizzo et al. showed that the average number of hydrogen bonds for $-NH_2$ group is 2.51 [28]. On the other hand, from MD simulations, Meng et al. showed that 1.77 hydrogen bonds were possible between amine and water molecules [16]. According to the reference interaction site model (RISM) calculations, 2.4 hydrogen bonds are present per amine group [29]. Lozano et al. applied density functional theory (DFT) calculations on water-methylamine clusters and showed that the strength of the NH_2-water hydrogen bonds increased with increase in the size of the cluster [30]. Biswas et al. applied the first principle molecular dynamics on an aqueous solution of MA to explore hydrogen bond dynamics and vibrational spectral diffusion. They showed that the amine group formed 2.5 hydrogen bonds with water [19]. The carboxylate functional group plays a significant role in biology; at least one $-COOH$ group is present in all amino acids. Calculating the structure and dynamics of carboxylate groups, along with ammonium ions, will provide useful information about the behavior of biological species in aqueous solutions [31,32]. $RCOO^-$ has a polar head group which interacts with surfactant molecules and forms vesicles and missiles [33,34]. Although it is important, very little experimental work on hydration structure of the simple caroboxylate group, formate (FMT) ion, was reported [35–37]. The structural information about FMT ion was obtained from computer simulations using different molecular force fields [32]. Jorgensen and Gao applied MC techniques with the use of OPLS force fields for FMT and acetate ions. They found that hydration numbers for formate and acetate were 3.6 and 3.4, respectively [15]. Alagona et al. used TIP4P model for water to report structural properties and found a slightly lower hydration number 3 for acetate ion and 3.4 for FMT ion. Due to the steric hindrance of the methyl group in acetate, it tends to accommodate the lower number of water molecules than FMT ion [9]. Similar results were obtained using SPC/E [16,38] model for water, which predicted hydration number of 3.3 for acetate. However, when polarizable force field POL3, this number dropped slightly to 3.1 [39]. The reported studies mainly concentrate on the structure of ions in hydrated conditions. Dynamics of hydrogen bonding of these systems is not well studied.

The main aim of this manuscript is to understand the solvation behavior of water around methyl ammonium and formate ions as well as the corresponding conjugate neutral molecules both in dilute and concentrated aqueous solutions to quantify the extend of hydrogen bonding of water molecules with the solutes. So, we calculated various structural aspects as well as the hydrogen bond dynamics of the involved pairs. The lifetimes of hydrogen bonds in aqueous solution were calculated from corresponding continuous correlation function by defining the H-bonded and non-bonded states based on geometric criteria obtained from radial distribution functions. The focus is to observe the transformation of structural and hydrogen bond dynamic properties from neutral molecules to charged ions in both dilute and concentrated aqueous solutions. Although many studies have been reported on formate, acetate, methylamine and methylammonium ions in aqueous solutions, no study was reported on an aqueous solution of MAF ionic pair in water and the comparison of single MAF with a bulk aqueous solution of MAF. To fill this gap, here, structure and dynamics of MAM

Table 1
Information about simulated Systems.

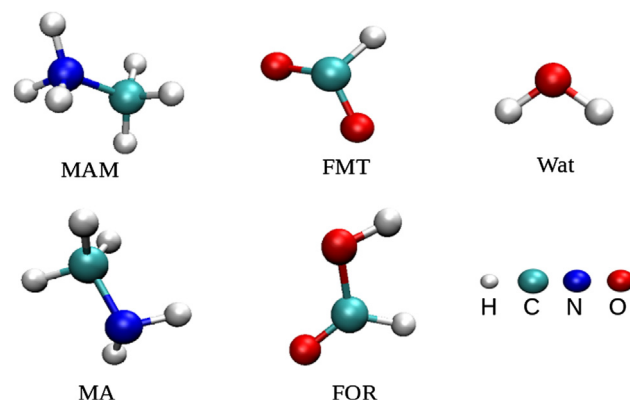|	MAM	FMT	MA	FOR	Water
System 1	1	1	–	–	1000
System 2	250	250	–	–	750
System 3	–	–	1	–	1000
System 4	–	–	250	–	750
System 5	–	–	–	1	1000
System 6	–	–	–	250	750

Fig. 1. Chemical structures of ions or molecules used in this study. MAM = methylammonium cation, FMT = Formate anion, MA = methylamine, FOR = formic acid, Wat = water.

and FMT ions of MAF, neutral molecules like MA and FOR were studied in both dilute and concentrated aqueous solutions.

2. Models and simulation details

We performed six different simulations; three simulations of single solutes (MAF, MA and FOR) in 1000 water molecules and another three simulations of 250 solutes (MAF, MA and FOR) in 750 water molecules. The details of the systems are given in Table 1. All simulations were carried out using GROMACS program [40–42]. Chemical structures of solutes and solvent are shown in Fig. 1. Fixed charge water model SPC/E was used in this study [16,38]. Single ion or molecule was optimized in Gaussian software with the use of B3LYP/6-311 + G(2d, p) method [43]. Optimized ions/molecules were replicated using Packmol software [44]. Antechamber package was used to generate partial charges [45]. Optimized Potentials for Liquid Simulations-all atoms (OPLS-AA) force field was used for the MAF, MA and FOR [46]. The force fields were generated using the MKTOP program [47]. Nonbonding parameters were presented in Table S1. Steepest descent method was used for the initial energy minimization [48]. A simulation of 2 ns was performed in the NVT ensemble at higher temperatures to get proper mixing of ions/molecules. Annealing process was applied for 1 ns to cool down the system to room temperature. 10 ns simulation was performed in the *NpT* ensemble at room temperature. Last 8 ns trajectory was used to calculate the density. Subsequently, the equilibration was done in the NVT ensemble for 10 ns at room temperature. The V-rescale thermostat and Berendsen barostat was used during the equilibration with coupling constants of 0.1 and 2.0 ps, respectively [49,50]. Periodic boundary conditions in three dimensions were used to ensure the bulk limit. Long-range electrostatics was treated with particle mesh Ewald (PME) method with the cut-off value of 1.2 nm. The cut-off value for nonbonded interactions was used as 1.2 nm. Equations of motion were integrated with the use of velocity–Verlet algorithm. LINC algorithm was used to constrain the bonds of hydrogen atoms. 40 ns production run was performed in the NVE ensemble and the obtained trajectories were used for further analysis.
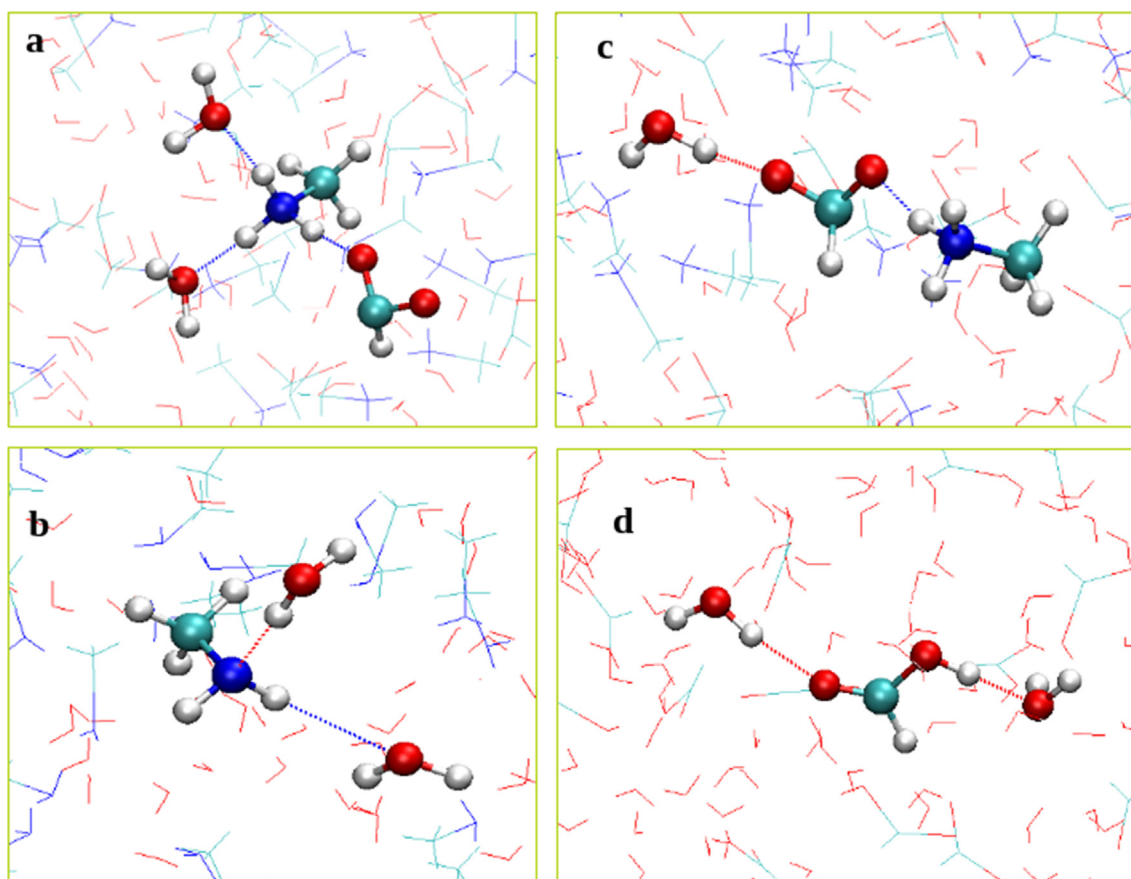
Fig. 2. Snapshots of different possible hydrogen bonding environments around the molecules or ions. Figures a and b are from the concentrated solutions of MAF and MA, respectively. Figures c and d are from concentrated solutions of MAF and FOR, respectively. Dashed lines indicate hydrogen bonds.

3. Results and discussion

3.1. Solvation structure

In Fig. 2a and b, we show how MAM (System 2) and MA (System 4) are interacting with water. These figures show the main differences between the structure of hydrogen bonding around cation and its conjugate neutral form. Similar structures were observed around ammonia and ammonium ion in aqueous solutions by Ekimova et al. [51] According to this study, ammonia forms only one strong hydrogen bond through its nitrogen atom, which accepts a hydrogen bond. Three hydrogen atoms of ammonia are not coordinated by water molecules most of the time. On the other hand, ammonium ion forms four hydrogen bonds through its hydrogen atoms by donating. Our study also shows that MA forms hydrogen bonds mainly through its nitrogen atom by donating and MAM forms three strong hydrogen bonds as hydrogen bond donor in aqueous solution. In MAM, all three N−H groups act as hydrogen bond donating groups. MA molecule acts as a hydrogen bond acceptor by forming H−O−H…NH_2 bond. In Fig. 3a and d, we have compared the similar interactions of neutral and conjugate forms. From Fig. 3a, the oxygen atom of water interacts strongly with the ammonium hydrogen atoms (H_N) of MAM. In this study, oxygen and hydrogen atoms of water are designated by a subscript 'w'. The first peak of O_w−H_N is found at 0.174 nm. Number integrals reveal that MAM is surrounded by more number of water molecules in diluted condition. The first peak of O_w−H_N RDF of MA is found at 0.210 nm. The position of peaks in RDFs is independent of dilution. Hydrogen bonding between O_w with H_N atoms is similar in both diluted and concentrated solutions. Hydrogen bonding between H_N and O_w in aqueous solution of MA is weak, and possibility of these types of hydrogen bonds is rare. On the

other hand, the hydrogen bonding between N and H_w in aqueous MA (Fig. 3c) is strong and can be compared to O_w−H_N hydrogen bonding in aqueous MAM. The first peak position of N−H_w is found at 0.190 nm in aqueous MA. This distance is slightly larger than in O_w−H_N in MAM. The structure of second solvation shells is similar in both the aqueous solutions of MAM and MA. Ionic form shows well-defined second solvation shell than Neutral forms. Fig. 2c and d show the solvation structure around FMT anion and formic acid, respectively. FMT anion can form strong hydrogen bonds with both water and ammonium ion. FMT anion accepts the hydrogen bond, whereas, in aqueous solution, formic acid acts as both hydrogen bond donor and acceptor. We have also observed the solvent separated ion pair in system 2 and present in Fig. S1. The structure around the formic acid and FMT ion is further investigated by RDFs. Fig. 3d compares the all-possible interactions between oxygen and acidic hydrogen atoms except O_w−H_N and H_N−O_{FMT}. The oxygen atom of FMT anion strongly interacts with hydrogen atoms of water. Interestingly, oxygen atom of water also shows strong affinity towards hydroxyl hydrogen atom of formic acid, which competes with O_{FMT}−H_w interaction. Further, the local environment in the second solvation shell around the formic acid and FMT anion has a similar structure. The RDFs between the carbonyl oxygen of formic acid and hydrogen of water show different behavior. The first solvation shell of the formic acid is poorly coordinated around carbonyl oxygen as compared to the hydroxyl group of formic acid. The carbonyl oxygen atom of formic acid (O_{FOR}) has less affinity towards the water molecules as compared to O_{FMT}. Overall, the MAM cation forms relatively strong hydrogen bonds through its three hydrogen atoms with water. MA forms weak hydrogen bonds with water through nitrogen atom. These results are consistent with previous studies on ammonium ion and amine [51]. Hydrogen bonding between cation and anion are the
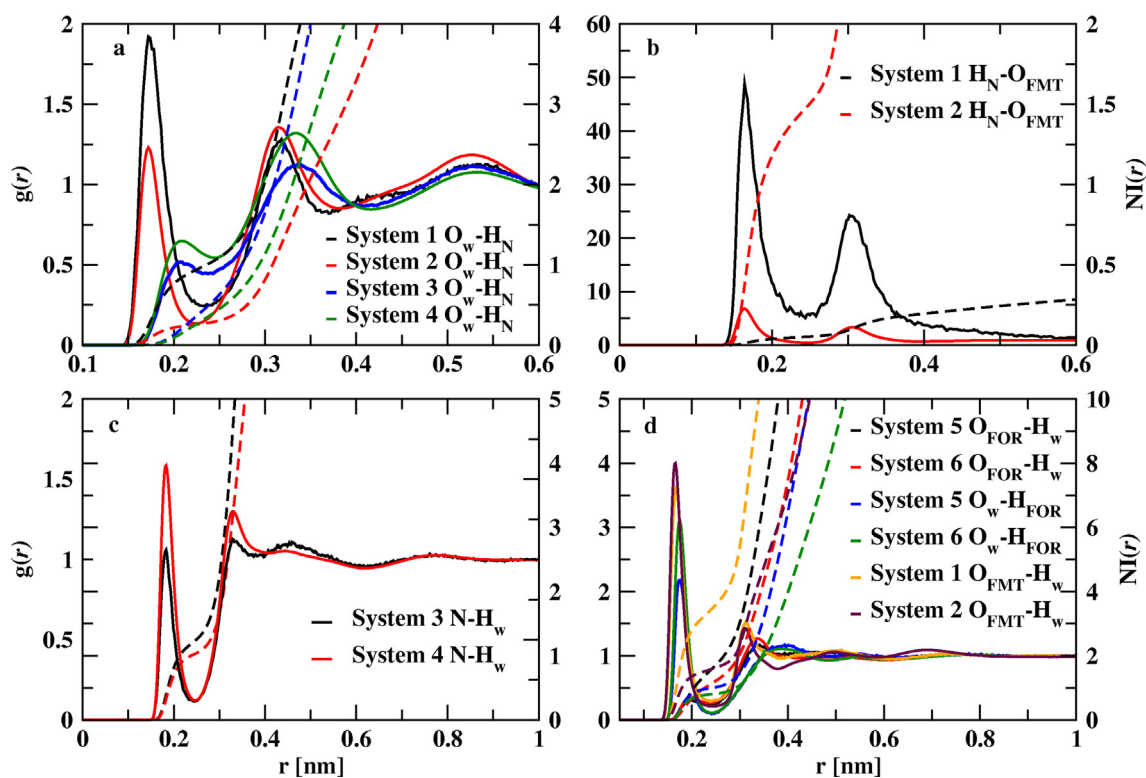
Fig. 3. Atomic radial distribution functions between O and H atoms. System 1 = Diluted MAF, System 2 = Concentrated MAF, System 3 = Diluted MA, System 4 = Concentrated MA, System 5 = Diluted FOR, and System 6 = Concentrated FOR.

strongest among all the interactions. $O_{FOR}-H_w$ correlation is weaker than O_w-H_{FOR} pair. Formic acid approaches water through its hydroxyl hydrogen atom rather than carbonyl oxygen atom.

RDF between O_w and H_N are shown in Fig. 3a. RDFs between the carbonyl oxygen of FMT anion (O_{FMT}) and hydrogen atoms of water (H_w) (Fig. 3d) show stronger interaction than that between the oxygen of water (O_w) and the hydrogen of the amine group (H_N) in MA. The position of the first peak for $O_{FMT}-H_w$ RDF is found at 0.167 nm and for O_w-H_N RDF is at 0.177 nm. In ionic environment, O_{FMT} and H_w come closer than O_w and H_N. The first minima of distribution functions are found around 0.246 nm. More peak heights of $O_{FMT}-H_w$ RDFs suggest that hydrogen bonding between FMT ion and water in aqueous MAF is stronger as compared to MA…water hydrogen bonding. These interactions are slightly influenced by the concentration of ionic liquid (MAF). Heights of the second peaks of all these RDFs are equal and show the second minima at the same position. The main features of all these RDFs (Fig. 3a) are matching with those derived from previous QM/MM studies [52–54]. For instance, the position of first peaks of $O_{FMT}-H_w$ was found at 1.710 nm. Our results are in good agreement with classical and MC simulations [9,15,16]. The interaction decreases from Wat–FMT to Wat–MA. The hydrogen atom of water is attached to more electronegative oxygen atom in the former case but in case of Wat-MA, hydrogen of ammonium group attached to less electronegative nitrogen atom than oxygen which makes interaction weak. In diluted MAF, O_w interacts strongly with the hydrogen atom of the ammonium group than in concentrated solution, whereas, O_{FMT} shows strong interaction with H_w in concentrated MAF than diluted one. Interactions between ion pairs of MAF were studied by calculating the RDFs between the hydrogen atoms of ammonium (H_N) and oxygen atoms of FMT (O_{FMT}) in diluted and concentrated solutions (Fig. 3b). Interestingly, the ion-pair interaction between cation and anion is more at the diluted condition. This can be due to facilitation of well-defined solvation environment between water molecules as two ions come closer. According to Fig. 3b, the first H_N-O_{FMT} RDF peak is found at

0.167 nm, which is similar to $O_{FMT}-H_w$ RDF (Fig. 3d). Even though the peak positions are equal for these two types of RDFs, peak heights differ much. This is due to existing strong electrostatic and hydrogen bonding interactions between opposite ions of MAF. Formate anion forms strong hydrogen bonds with water molecules through its oxygen atoms. The hydrogen bonding between ion pairs is the strongest due to the opposite charges on ions. H_N-O_{FMT} pair shows strongest correlation than any other pairs in this study. Water molecules come close to the ions as compared to their corresponding neutral conjugate forms. In Fig. 3a, we observe a small peak at 0.210 nm in O_w-H_N RDF followed by a pronounced peak at 0.340 nm for the MA system. A third peak is also recognizable at 0.540 nm. These RDFs reveal that the interaction of water with the neutral molecule, MA, is less as compared to ionic species. RDFs of $O_{FOR}-H_w$, and O_w-H_{FOR} pairs were calculated in formic acid and water mixture for both diluted and concentrated conditions. $O_{FOR}-H_w$ RDF shows the broad first peak at 0.200 nm and pronounced second peak at 0.340 nm (Fig. 3d). First solvation shell of O_w-H_{FOR} corresponds to a sharp first peak at 0.180 nm and a broad second peak at 0.380 nm. These O_w-H_{FOR} RDFs indicate strong interactions between acidic hydrogen of formic acid and oxygen of water. From these two types of RDFs (Fig. 3d); formic acid approaches the water molecule preferentially through its acidic hydrogen atom rather than its carbonyl oxygen atom. With the change in concentration of MAF, peak positions do not change. However, a change in peak height with the variation of concentration of MAF is observed. The solvation structure of hydroxyl group and carbonyl group is different for formic acid.

Center of mass (COM) RDFs and corresponding number integrals are shown in Fig. S2. Not much difference is found between water−water RDFs with concentration change or ionic to a neutral environment. The first peak represents the interaction between amine or ammonium hydrogen atoms and O_w. As the environment changes from ionic to neutral, heights of the first and second peaks decrease. No change in peak position is observed when the environment changes. Wat−FOR/FMT

COM RDFs reveal that interactions of FMT anion with water are stronger as compared to formic acid and water. The heights of the first peak decrease from FMT anion to formic acid. The water molecules which are present near to FMT anion form strong hydrogen bonds with FMT. FMT anion shows the correlations till third solvation shell, which cannot be found with formic acid. The long-range interaction of FMT anion and the formation of aggregate-like structures in the ionic environment are possible. The complexes formed around the ions and hydrogen bonding by FMT ion tend to slow down the dynamics of ionic solutions when compared to pure solvents. These results show that ion-dipole interactions are much stronger than dipole-dipole interactions. Cluster-like environment is possible around the charged particles that leads to slower dynamics.

Coordination numbers (CN) were calculated from the COM RDFs by considering their first minima. CNs are presented in Table S2. CN of water around FMT ion in diluted and concentrated MAF is found to be 8.10 and 3.60, respectively [9]. From the previous studies, it was found that the hydration numbers of FMT are 3.60 and 3.40 [16,38]. CN for Wat–Wat is found to be 4.40 in diluted MAF and 2.40 in concentrated solution. Aqueous solutions of neutral forms, formic acid, and MA also show a decrease in coordination number with the increase in the concentration of formic acid/MA. For example, in formic acid Wat-Wat coordination number in diluted condition is found to be 4.32 and is decreased to 3.44 in concentrated solution. In diluted condition, four water molecules are present in the first solvation shell of MAM cation. When the concentration of MAF is increased, coordination number decreases from 4.25 to 1.62. CNs of neutral species (MAM/FOR) are found to be large (Table S2) which is due to the extended first solvation shell. The number of water molecules in the first solvation shells of ions/molecules are higher for diluted solutions than the corresponding concentrated solutions. When concentration increases, the ions or molecules replace the water molecules in the first solvation shell.

Spatial distribution functions (SDFs) of water molecules around ions/molecules were calculated to investigate the three-dimensional distribution of solvent molecules (Fig. 4) using TRAVIS software package [55]. From Fig. 4a, the oxygen atoms of water molecules orient around three hydrogen atoms of the ammonium group in MAM. This behavior is also observed from the RDF between MAM cation and water (Fig. 3a). Fig. 2a also shows that the three acidic hydrogen atoms of MAM form hydrogen bonds with neighbor molecules/ions. Fig. 4b

shows the distribution of water molecules around the MAM cation in concentrated aqueous MAF solution. The distribution of water around MAM is different from the diluted solution, which is due to the presence of other ions in the first solvation shell. However, the oxygen atoms of water molecules are found to be around hydrogen atoms of ammonium which is similar to diluted condition. Water molecules approach towards acidic hydrogen atoms of MAM cation. The water around MA (Fig. 4g, h) shows different structure compared to MAM. The nitrogen atom of MA interacts with hydrogen atoms of water strongly, which is consistent with previous results [51]. The oxygen atom of water molecule interacts with the acidic hydrogen atoms of MAM cation. Fig. 2a and b show similar results. There are two possible sites in FMT (Fig. 4c, d) to form hydrogen bonding with water molecules. Water molecules are found to stay in the proximity of two oxygen atoms of FMT anion. The distribution of water around neutral species (MA and FOR) and ionic species is different and also different in dilute and concentrated solutions. As expected, the probability of finding water around FOR is found to be higher at two different sites. Hydrogen atoms of water are oriented towards carbonyl oxygen atom of FOR, and the oxygen atoms of water are situated around acidic hydrogen of FOR. Distribution of water around formic acid is slightly different. In Fig. 4g and h, SDFs of water have similar characteristics, and the only difference is a slight distraction of SDF in diluted condition. Oxygen atoms of water molecules preferentially locate around the hydrogen atoms of MA, whereas hydrogen atoms of water preferentially locate around nitrogen atom of MA. The visualization of differences in the distribution of atoms of water around given ions/molecules allows us to interpret the interaction of water with ions/molecules at the atomic level. Results from spatial distribution functions support the RDFs that the interactions are directional in nature.

Combined distribution functions (CDFs) were calculated using RDF and angular distribution function (ADF) with the use of TRAVIS software (Figs. 5 and S3) [55]. Figs. 5 and S3 represent the similar interactions in concentrated and dilute solutions, respectively. Fig. 5a is obtained by combining the H_N-O_w distances and $N-H_N...O_w$ angle in concentrated MA. At larger distances, no change is observed in the ADF due to absence of preferred orientation. The oxygen atoms of water molecules are located near acidic hydrogen atoms of MA. This finding is in agreement with the RDFs and SDFs. The preferred H_N-O_w distance is around 200 pm, which corresponds to the oxygen of water that is close
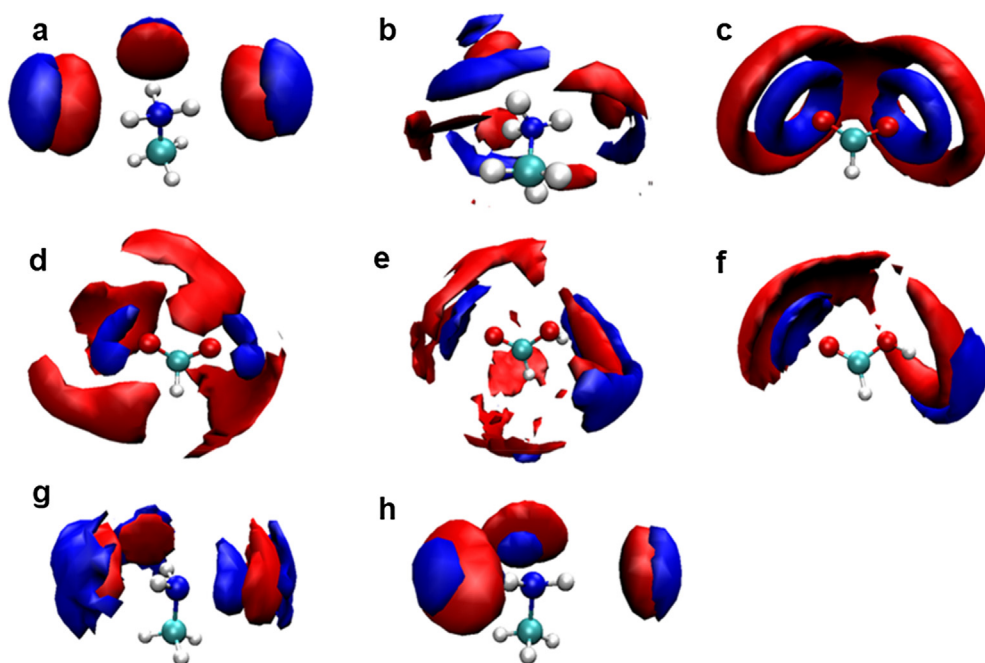

Fig. 4. Spatial distribution functions of hydrogen (blue) and oxygen (red) atoms of water molecule around the solute particles. a. The water around MAM in diluted condition, b. The water around MAM in concentrated condition. c. The water around FMT anion in diluted condition, d. The water around FMT anion in concentrated condition. e. The water around FOR in diluted condition. f. The water around FOR in concentrated condition. g. The water around MA in diluted condition. h. The water around MA in concentrated condition. (For interpretation of the references to colour in this figure legend, the reader is referred to the web version of this article.)
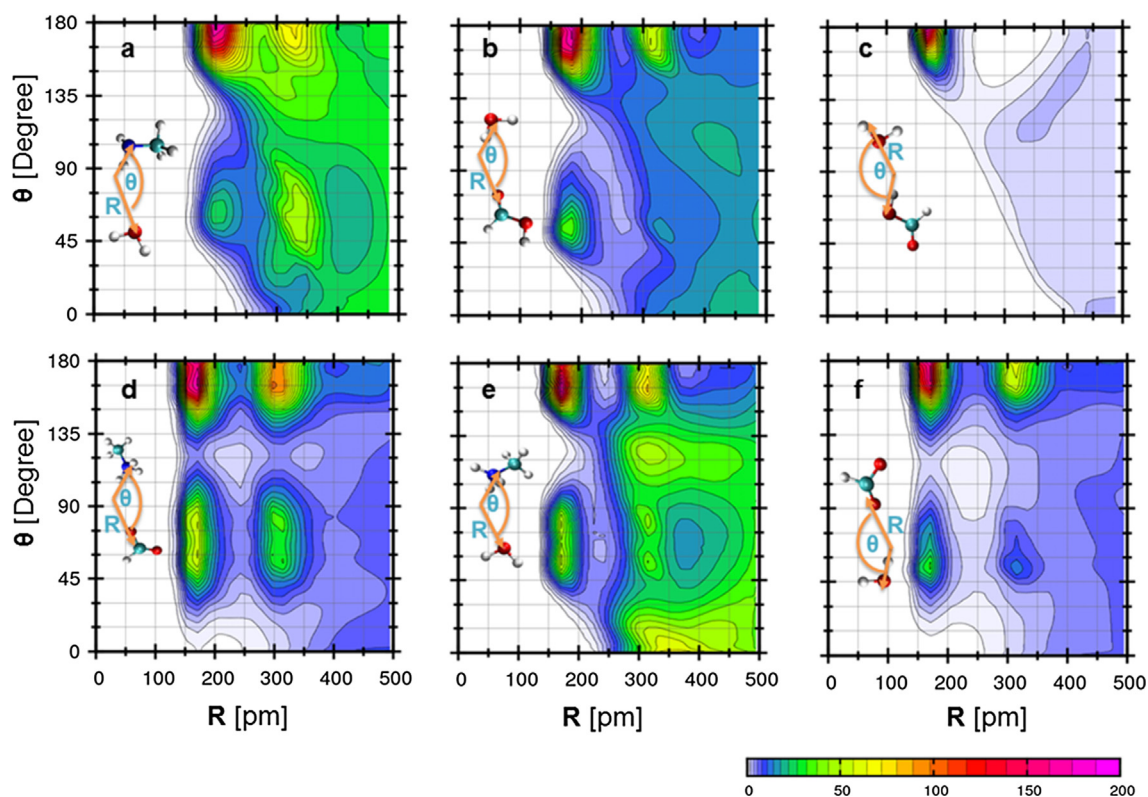
Fig. 5. Combined distribution functions of RDF and ADF between the molecules/ions in concentrated aqueous solutions. The X-axis indicates RDF and Y-axis indicates ADF in the plots. The angle considered here represents the hydrogen bond angle. Models for distance and angle were shown in the respective fig. itself. Models are presented in the figures. The top row indicates the CDFs between water and neutral species. The bottom row indicates the CDFs between different possible pairs in concentrated MAF. a. CDF between the H_N-O_W distances and the $N-H_N-O_w$ angles. b. CDF between the H_w-O_{FOR} distances and the $O_w-H_w-O_{FOR}$ angles c. CDF between the $H_{FOR}-O_w$ distances and the $O_{FOR}-H_{FOR}-O_w$ angles. d. CDF between the H_N-O_{FMT} distances and the $N-H_N-O_{FMT}$ angles. e. CDF between the H_N-O_{FMT} distances and the $N-H_N-O_{FMT}$ angles. e. CDF between the H_N-O_W distances and the $N-H_N-O_w$ angles. f. CDF between the H_w-O_{FMT} distances and the $O_w-H_w-O_{FMT}$ angles.

to the H_N of the amine group. In this configuration, a hydrogen bond is formed between H_N and O_w with hydrogen bond angle as around 180°. Another peak is observed in the RDF of H_N-O_w around 350 pm, which corresponds to the second solvation shell. For formic acid, two types of hydrogen bonds are possible. Fig. 4b corresponds to one type (H_w-O_{FOR}), and Fig. 4c corresponds to another type (O_w-H_{FOR}). Model representations for defining angle and distance were shown inside the figure. H_w-O_{FOR} CDF features three distinguishable peaks in RDF. Among two peaks around 180°, one peak corresponds to the distance of 170 pm, and another one is at 350 pm due to existence of the long-range interactions. The third peak around 45° is due to the interaction between H_w and oxygen of the hydroxyl group in formic acid. $H_{FOR}-O_w$ CDF (Fig. 5c) has only one peak corresponding to 180° angle and 190 pm distance, which shows preferential occupation of H_{FOR} towards O_w. At longer distances, no distribution is found. This kind of distribution is not observed for other systems. Three types of hydrogen bonds are possible in MAF systems. These are shown in Fig. 5d, e, and f. We can see the maximum at an expected distance of 170 pm, located at 180° angle. CDFs of MAM–Wat and FMT–Wat are given in Fig. 5e and f. We investigate the CDF of the angle between H_N-N and H_N-O_w vectors and the distance axis defined between H_N and O_w. The angular axis depicts the angle between two vectors. In Fig. 5e. maximum is found at 200 pm distance and 180° angle. Similarly, in Fig. 5f, the most probable angle is found at 180°. In all the CDFs hydrogen bonds are found to be close to linear and the most probable hydrogen bond distance is found below 210 pm. We have also calculated the CDFs for corresponding diluted solutions and are shown in Fig. S3. Both diluted and concentrated solutions show similar CDFs for the same type of interactions. The structure of water around solutes does not change with

concentration. From Fig. 2a, O_w atoms stay near acidic hydrogen atom of MA. All the hydrogen bonds are linear in nature in this study. H_{FOR} preferentially occupies the solvation shell of O_w. The CDFs between MAM and FMT show two possible angles at two different distances in which linear hydrogen bonds dominate.

3.2. Hydrogen bond and residence dynamics

After looking at the structure of the hydrogen bond of the protic ionic pair and their conjugate forms, it is intuitive to explore the dynamics of possible hydrogen-bonded pairs and residence dynamics of water molecules in the solvation shell of charged ions as well as neutral molecules. We calculated the hydrogen bond autocorrelation function [56–58] defined as

$$C_{HB}(t) = \frac{<h(0)h(t)>}{<h^2(0)>} \quad (1)$$

The probability of two molecules remains hydrogen-bonded at time t given by considering that they were hydrogen-bonded at initial conditions. The functions h(t) represents the specific hydrogen-bonded pairs having values of 0 or 1. Thus $C_{HB}(t)$ allows breaking and making of hydrogen bonds. The cutoff distance for the hydrogen bonds is the corresponding minimum in RDF. Also, we have also calculated the hydrogen bond forward lifetimes and continuous HB lifetimes. The time dependence of correlation functions is shown in Fig. 6. HB forward and continuous HB lifetimes are presented in Table S3. As forward lifetimes depend on intermittent HB correlation functions, continuous lifetimes are much lower than forward lifetimes. Water…water (Wat…Wat) hydrogen bond autocorrelation functions reveal that the decay in diluted conditions is identical. Forward lifetime of Wat…Wat is found to be around 3.98 ps and continuous lifetimes were found to be around
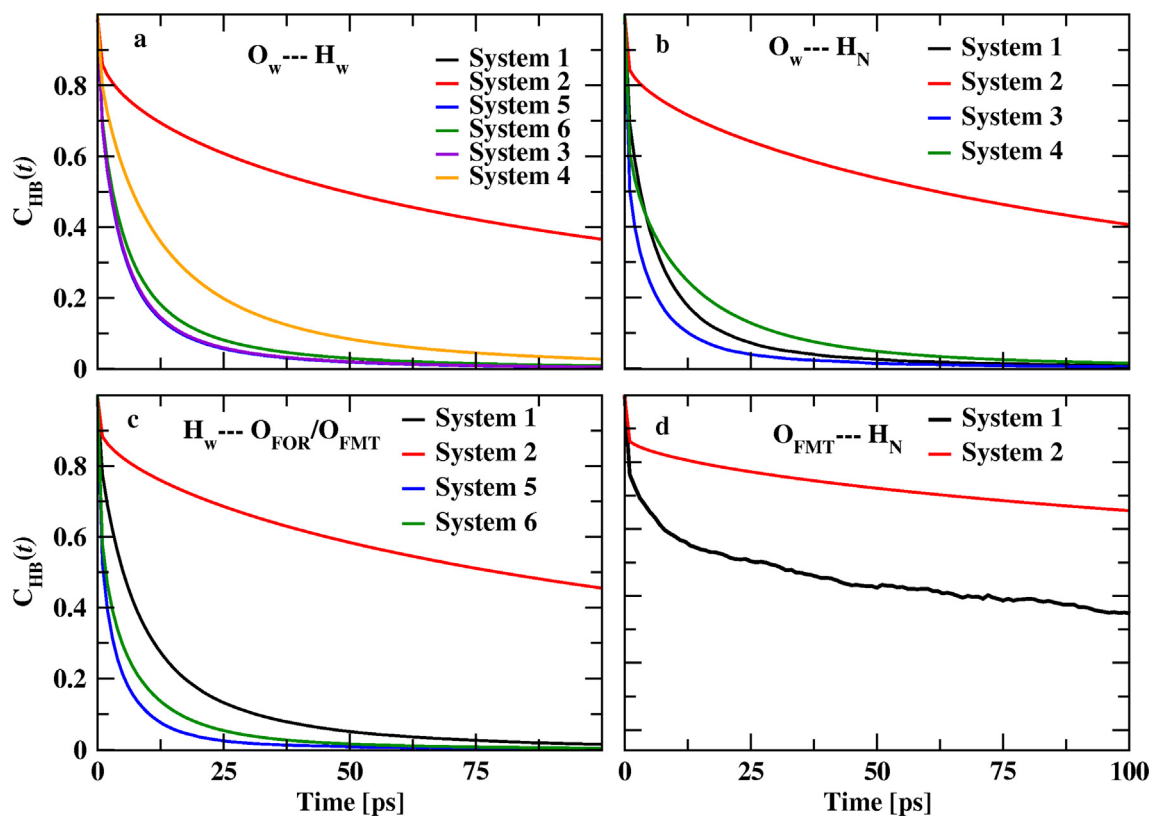
Fig. 6. Hydrogen bond autocorrelation functions of Water-Water(Wat-Wat), Wat-MA/MAM, Wat-FOR/FMT, and MAM-FMT. Systems are described in Fig. 2.

0.51 ps which are consistent with earlier studies of pure water [59–61]. The presence of only single solute in 1000 water molecules does not make a difference in the dynamics of Wat…Wat hydrogen bonds. Unlike the diluted case, the decay is slower in concentrated solutions. Concentrated MAF solution shows the slowest decay. These results ascertain that the stronger ion-ion and ion-water correlations in the ionic environment. Forward lifetimes for Wat…Wat is 37.7 ps and continuous lifetime is 0.9 ps which are much higher than diluted condition. The ionic environment promotes strong Wat…Wat hydrogen bonds. This is in agreement with the COM RDF of Wat–Wat in MAF. The first peak height of Wat–Wat RDF increases in concentrated MAF than in diluted condition. The next slowest decay is found for concentrated MA. Wat… Wat forward lifetime for the concentrated solution is found to be 8.24 ps and continuous lifetime is 0.73 ps. The deviation of Wat…Wat HB autocorrelation function in concentrated formic acid is very less from diluted: forward lifetime is 4.33 ps and continuous lifetime is 0.52 ps. These lifetimes are close to diluted Wat…Wat lifetime. Therefore, the concentrated formic acid has less effect on water dynamics than MA and MAF. This effect can be seen from the COM RDFs, where Wat-Wat interaction is low among all the concentrated solutions. Wat…MA/MAM autocorrelation functions show the slowest decay for concentrated MAF. In the ionic environment, due to ion-ion interactions, decays are very slow. Concentrated MAF shows continuous HB lifetime of 0.65 ps and a forward lifetime of 66.64 ps for Wat-MAM, whereas diluted MAF shows continuous and forward lifetimes as 0.51 and 6.14 ps respectively. This behavior also correlates to the results obtained from the CDF, where concentrated MAF shows more correlation than diluted. In diluted MA/MAF, the decay is very fast, which shows the faster breaking and making of HBs. Similar results are observed from Wat…FOR/FMT decays. MAM…FMT autocorrelation functions show the slowest decay among all the calculated pairs due to the electrostatic attraction between opposite ions and the strong hydrogen bonding. Here we note that the RDFs and CDFs between MAM and FMT also show that MAM…FMT correlations are the strongest.

Neutral forms show relatively less hydrogen bond lifetimes than corresponding ionic forms. The concentration of MAF and MA affects the dynamics of water-water hydrogen bonding, whereas no change in structure is observed from COM RDFs. On the other hand formic acid has negligible effect on both structure and dynamics of water-water hydrogen bonds. The dynamics are the slowest in ionic environment. MA shows the second slowest decay for water-water hydrogen bond dynamics correlation function. MAM-FMT correlation is the strongest and agree well with CDF and RDF results.

We have calculated residence times by constructing the time autocorrelation function $C_{Res}(t)$ [62]. The residence times give information about the time spent by an atom or molecule within a given distance. $C_{Res}(t)$ is defined as

$$C_{Res}(t) = \frac{<g(0)g(t)>}{<g(0)^2>} \qquad (2)$$

where $g(t)$ indicates the residence population variable. If the molecules are present in the given distance cutoff value, then $g(t)$ is considered as one; otherwise, it is zero. $g(t)$ is calculated according to the intermittent definition. The molecule/ions can enter and leave the first solvation shell during the calculation. Residence times were calculated between COM of water and the solutes to see how much time water molecules stay in the first solvation shell. The bi-exponential function was used to fit the decay of $C_{Res}(t)$

$$C_{Res}(t) = A\exp\left(-\left(\frac{t}{\tau_1}\right)^{b1}\right) + (1 - A)\exp\left(-\left(\frac{t}{\tau_2}\right)^{b2}\right)\ldots\ldots \qquad (3)$$

Distance cutoff values were considered from the first minima of COM RDFs. Fitted parameters are presented in Table S4. Diluted solutions show lower residence times as compared to concentrated. This is due to increased viscosity and ion-pair as well as ion-dipole interactions. For example, MAM shows 84.120 ps residence time in diluted condition, but in concentrated, it raises to 398.267. This behavior is

already observed from the hydrogen bond dynamics. Neutral forms show less variance of residence times with change in concentration of solute. The residence times of MA in diluted and concentrated conditions are 135.581 and 194.757 ps, respectively. The lack of strong electrostatic and hydrogen-bonding interactions plays a vital role in concentrated solutions of neutral molecules. The residence time of water around MAM cation is 398.267 ps as compared to MA(194.757 ps) in concentrated solutions. FMT ion and formic acid show 307.577 ps and 75.787 ps residence times of water molecules, respectively. Water spends more time near the ionic species than neutral molecules as the concentrated solutions have slower dynamics than corresponding diluted solutions.

4. Summary and conclusions

In the present study, we explored the structural and dynamical aspects of the aqueous solution of MAF, MA, and FOR to have a comparative investigation that how MAF and its conjugate neutral forms interact with water. We also performed simulations of diluted and concentrated solutions to compare bulk properties with single-particle properties. It is found that the MAM cations have strong interaction towards the FMT anion in aqueous solution. Ammonium hydrogen atoms of MAM cation interact the FMT anions through oxygen atoms. The solvation shells of these ions (MAM and FMT) are also well structured due to the existing strong hydrogen bonding and ion-dipole interactions. Solvation shell of neutral molecules (MA and FOR) is not as well defined as that of ions. Even though the difference between MA and MAM is a single proton, their solvation environments are different. MAM favors the hydrogen bond through its protons towards the O_w and MA tends to form strong hydrogen bond through its nitrogen atom with water. These features can be seen from the RDFs and CDFs. SDFs reveal the interacting sites in solutes towards the water molecules. SDFs were used to show the preferred location of hydrogen and oxygen atoms of water molecules around solute particles. The distribution of water around solute is similar in dilute and concentrated solutions. However, the dynamics of hydrogen bonds are different in diluted and concentrated solutions. The concentration of ions/molecules does not affect the structure but dynamics. Hydrogen bonding between water molecules shows higher lifetimes in concentrated solutions as compared to diluted solutions. Increasing the concentration of ions/molecules promotes the hydrogen bonding between water molecules. From the calculations of residence dynamics, it is found that the water molecules stay more time near ionic entities rather than neutral molecules. Moreover, their forward and continuous lifetimes of hydrogen bonds are longer in the ionic environment. A transition of dynamics can be observed from diluted to concentrated condition. Forward lifetimes are found to be highest between opposite ions in aqueous MAF. Not much change in wat-wat structure and dynamics is observed in dilute solutions. The residence time of water around solute molecules was found to be high in concentrated MAF due to existing strong ion-ion and ion-dipole interactions.

CRediT authorship contribution statement

Th. Dhileep N. Reddy: Investigation, Formal analysis, Visualization, Validation, Writing - original draft. **Bhabani S. Mallik:** Conceptualization, Methodology, Writing - review & editing, Supervision, Project administration, Funding acquisition.

Declaration of Competing Interest

The authors declare that they have no known competing financial interests or personal relationships that could have appeared to influence the work reported in this paper.

Acknowledgements

Appendix A. Supplementary material

Supplementary data to this article can be found online at https://doi.org/10.1016/j.comptc.2019.112663.

References

[1] P.G. Wolynes, Annu. Rev. Phys. Chem. 31 (1980) 345–376.
[2] O.A. Karim, J. Andrew McCammon, J. Am. Chem. Soc. 108 (1986) 1762–1766.
[3] H. Eggerer, R. Huber (Eds.), Structural and Functional Aspects of Enzyme Catalysis: 32. Colloquium, 23. - 25. April 1981, Springer-Verlag, Berlin Heidelberg, 1981.
[4] A. Späth, B. König, Beilstein J. Org. Chem. 6 (2010) 32.
[5] J.A. Gingrich, M.G. Caron, Annu. Rev. Neurosci. 16 (1993) 299–321.
[6] O.S. Wolfbeis, H. Li, Biosens. Bioelectron. 8 (1993) 161–166.
[7] N.V. Plechkova, K.R. Seddon, Chem. Soc. Rev. 37 (2007) 123–150.
[8] J. Boyle, Biochem. Mol. Biol. Educ. 33 (2005) 74–75.
[9] Giuliano Alagona, Caterina Ghio, Peter Kollman, J. Am. Chem. Soc. 108 (1986) 185–191.
[10] G.N.J. Port, A. Pullman, Theor. Chim. Acta 31 (1973) 231–237.
[11] V. Vallet, M. Masella, Chem. Phys. Lett. 618 (2015) 168–173.
[12] T. van Mourik, F.B. van Duijneveldt, J. Mol. Struct. THEOCHEM. 341 (1995) 63–73.
[13] K.-Y. Kim, W.-H. Han, U.-I. Cho, Y.T. Lee, D.W. Boo, Bull. Korean Chem. Soc. 27 (2006) 2028–2036.
[14] G.N. Chuev, M. Valiev, M.V. Fedotova, J. Chem. Theory Comput. 8 (2012) 1246–1254.
[15] W.L. Jorgensen, J. Gao, J. Phys. Chem. 90 (1986) 2174–2182.
[16] E.C. Meng, P.A. Kollman, J. Phys. Chem. 100 (1996) 11460–11470.
[17] H. Hesske, K. Gloe, J. Phys. Chem. A 111 (2007) 9848–9853.
[18] P. Chaiyasit, A. Tongraar, T. Kerdcharoen, Chem. Phys. 493 (2017) 91–101.
[19] S. Biswas, B.S. Mallik, Chem. Select. 2 (2017) 74–83.
[20] Y. Ding, D.N. Bernardo, K. Krogh-Jespersen, R.M. Levy, J. Phys. Chem. 99 (1995) 11575–11583.
[21] G.A. Lyles, S.A. McDougall, J. Pharm. Pharmacol. 41 (1989) 97–100.
[22] S. Baba, Y. Watanabe, F. Gejyo, M. Arakawa, Clin. Chim. Acta Int. J. Clin. Chem. 136 (1984) 49–56.
[23] A.M. Asatoor, D.N. Kerr, Clin. Chim. Acta Int. J. Clin. Chem. 6 (1961) 149–156.
[24] Y. Zhang, J. Mao, P.H. Yu, S. Xiao, Anal. Chim. Acta 752 (2012) 106–111.
[25] S. Xiao, P.H. Yu, Anal. Biochem. 384 (2009) 20–26.
[26] W.J. Dunn, P.I. Nagy, J. Phys. Chem. 94 (1990) 2099–2105.
[27] P.G. Kusalik, D. Bergman, A. Laaksonen, J. Chem. Phys. 113 (2000) 8036–8046.
[28] R.C. Rizzo, W.L. Jorgensen, J. Am. Chem. Soc. 121 (1999) 4827–4836.
[29] M.V. Fedotova, S.E. Kruchinin, Russ. Chem. Bull. 61 (2012) 240–247.
[30] M. Sánchez-Lozano, E.M. Cabaleiro-Lago, J.M. Hermida-Ramón, C.M. Estévez, Phys. Chem. Chem. Phys. 15 (2013) 18204–18216.
[31] I. Ivanov, M.L. Klein, J. Am. Chem. Soc. 124 (2002) 13380–13381.
[32] K. Leung, S.B. Rempe, J. Am. Chem. Soc. 126 (2004) 344–351.
[33] A. Ulman, An Introduction to Ultrathin Organic Films: From Langmuir-Blodgett to Self-Assembly, Academic Press, 2013.
[34] D.O. Shah, International Symposium on Micelles, Microemulsions, and Monolayers: Quarter Century Progress and New Horizons, eds., Micelles, Microemulsions, and Monolayers: Science and Technology, Dekker, New York, 1998.
[35] I.D. Kuntz, J. Am. Chem. Soc. 93 (1971) 514–516.
[36] Y. Kameda, T. Mori, T. Nishiyama, T. Usuki, O. Uemura, Bull. Chem. Soc. Jpn. 69 (1996) 1495–1504.
[37] Y. Kameda, K. Fukuhara, K. Mochiduki, H. Naganuma, T. Usuki, O. Uemura, J. Non-Cryst. Solids 312 (2002) 433–437.
[38] H.J.C. Berendsen, J.R. Grigera, T.P. Straatsma, J. Phys. Chem. 91 (1987) 6269–6271.
[39] J.W. Caldwell, P.A. Kollman, J. Phys. Chem. 99 (1995) 6208–6219.
[40] M.J. Abraham, T. Murtola, R. Schulz, S. Páll, J.C. Smith, B. Hess, E. Lindahl, SoftwareX 1–2 (2015) 19–25.
[41] H.J.C. Berendsen, D. van der Spoel, R. van Drunen, Comput. Phys. Commun. 91 (1995) 43–56.
[42] D. Van Der Spoel, E. Lindahl, B. Hess, G. Groenhof, A.E. Mark, H.J.C. Berendsen, J. Comput. Chem. 26 (2005) 1701–1718.
[43] M. Frisch, G.W. Trucks, H.B. Schlegel, G.E. Scuseria, M.A. Robb, J.R. Cheeseman, G. Scalmani, V. Barone, 464 B. Mennucci, G. ea Petersson, others, Gaussian 09, Gaussian, Inc. Wallingford, CT, 2009.
[44] L. Martínez, R. Andrade, E.G. Birgin, J.M. Martínez, J. Comput. Chem. 30 (2009) 2157–2164.
[45] J. Wang, W. Wang, P.A. Kollman, D.A. Case, J. Mol. Graph. Model. 25 (2006) 247–260.
[46] W.L. Jorgensen, D.S. Maxwell, J. Tirado-Rives, J. Am. Chem. Soc. 118 (1996) 11225–11236.
[47] A.A.S.T. Ribeiro, B.A.C. Horta, R.B. de Alencastro, J. Braz. Chem. Soc. 19 (2008) 1433–1435.

[48] M.C. Payne, M.P. Teter, D.C. Allan, T.A. Arias, J.D. Joannopoulos, Rev. Mod. Phys. 64 (1992) 1045–1097.

[49] H.J.C. Berendsen, J.P.M. Postma, W.F. van Gunsteren, A. DiNola, J.R. Haak, J. Chem. Phys. 81 (1984) 3684–3690.

[50] G. Bussi, D. Donadio, M. Parrinello, J. Chem. Phys. 126 (2007) 014101.

[51] M. Ekimova, W. Quevedo, Ł. Szyc, M. Iannuzzi, P. Wernet, M. Odelius, E.T.J. Nibbering, J. Am. Chem. Soc. 139 (2017) 12773–12783.

[52] C. Houriez, M. Meot-Ner (Mautner), M. Masella, J. Phys. Chem. B 119 (2015) 12094–12107.

[53] A. Payaka, A. Tongraar, B.M. Rode, J. Phys. Chem. A 113 (2009) 3291–3298.

[54] A. Payaka, A. Tongraar, B.M. Rode, J. Phys. Chem. A 114 (2010) 10443–10453.

[55] M. Brehm, B. Kirchner, J. Chem. Inf. Model. 51 (2011) 2007–2023.

[56] A. Luzar, D. Chandler, Nature 379 (1996) 55–57.

[57] A. Luzar, J. Chem. Phys. 113 (2000) 10663–10675.

[58] A. Chandra, Phys. Rev. Lett. 85 (2000) 768–771.

[59] J. Smiatek, J. Phys. Chem. B 118 (2014) 771–782.

[60] M.B. Hahn, T. Solomun, R. Wellhausen, S. Hermann, H. Seitz, S. Meyer, H.-J. Kunte, J. Zeman, F. Uhlig, J. Smiatek, H. Sturm, J. Phys. Chem. B 119 (2015) 15212–15220.

[61] G.S. Jas, E.C. Rentchler, A.M. Słowicka, J.R. Hermansen, C.K. Johnson, C.R. Middaugh, K. Kuczera, J. Phys. Chem. B 120 (2016) 3089–3099.

[62] B.S. Mallik, A. Chandra, J. Chem. Phys. 125 (2006) 234502.